JOURNAL OF SPACECRAFT AND ROCKETS
Vol. 35, No. 3, May–June 1998

Numerical Approach for Computing Noise-Induced Vibration from Launch Environments

Nickolas Vlahopoulos*
University of Michigan, Ann Arbor, Michigan 48109-2145
Charles Vallance†
GenCorp Aerojet, Sacramento, California 95813
and
Richard D. Stark III‡
Automated Analysis Corporation, Ann Arbor, Michigan 48104-6767

The development, implementation, and validation of a new numerical algorithm for predicting noise-induced vibration from acoustic loads experienced during launch vehicle liftoff are presented. The development is based on combination of boundary element and finite element technology. Two new important advancements are included and validated in this work: the existence of unequal mesh density between the structural and the acoustic model at their interface and the numerical simulation of a reverberant field as an acoustic environment. Results produced for an expanding nozzle of a rocket are compared successfully with test data. This development can be utilized during the initial and preliminary design phases of launch vehicles, when guidance can have significant impact.

Nomenclature

$[A]$ = boundary element (BE) matrix representing the primary system of linear equations
C = value of the integral associated with the derivation of the coupled matrices
$[C_1]$, $[C_2]$ = coupling matrices representing the effect of the structural vibration on the acoustic solution and the effect of the acoustic medium on the structural vibration, respectively
$\mathrm{d}\boldsymbol{F}$ = differential acoustic force exerted on a differential area $\mathrm{d}S$ of the structure
d_j = distance between acoustic node j and the ith node of the mth structural element
$\{F_a\}$ = forcing vector containing information about the acoustic excitation
$\{F_{\mathrm{St}}\}$ = mechanical load applied on the structure
$F(\phi)$ = quadratic functional
f = a known function
$[I]$ = identity matrix
$|J_{ml}|$ = Jacobian associated with of the lth integration point on the mth element
K_m = number of nodes in element m
L = number of integration points used within each element
M = number of elements in the structural finite element (FE) model
$N_k^m(l)$ = shape function associated with the kth node of the mth element, evaluated at the lth integration point
n = coordinate associated with the normal direction on the surface of the BE model
$\boldsymbol{n}$ = unit normal on the surface of the acoustic BE model; the side of the model toward the direction of the normal is defined as side 1, and the other as side 2
$\boldsymbol{n}_{ml}$ = unit normal associated with of the lth integration point on the mth element
p_1 = acoustic pressure on side 1 of the acoustic BE model
p_2 = acoustic pressure on side 2 of the acoustic BE model
$p(\boldsymbol{r})$ = acoustic pressure at location $\boldsymbol{r}$
R_i^m = number of closest nodes of the acoustic model to the ith node of the structural element m
RV = total number of acoustic waves comprising the reverberant excitation
$\Re(\phi)$ = operator on function ϕ
$\boldsymbol{r}$ = position vector
S = surface of the BE model
S_{St} = surface discretization associated with the FE model
$\{u_{\mathrm{St}}\}$ = structural degrees of freedom
$\boldsymbol{u}_{\mathrm{St}}$ = vector of structural displacement
$\boldsymbol{u}_{\mathrm{St}}(k, m)$ = structural displacement associated with the kth node of the mth element
$v(\boldsymbol{r})$ = acoustic velocity at location $\boldsymbol{r}$
w_{ml} = weighting factor associated with the lth integration point on the mth element
x_{ml} = location of the lth integration point on the mth element
$\delta p, \delta dp$ = primary variables defined on the surface of the acoustic BE model
$\{\delta p\}$ = vector of unknown primary variables on the surface of the BE model
$\delta p(i, m)$ = acoustic primary variable expressed on the ith node of the mth structural element
$(\partial p/\partial n)_1$ = normal gradient of the pressure on side 1 of the BE model
$(\partial p/\partial n)_2$ = normal gradient of the pressure on side 2 of the BE model
ρ = density of acoustic medium
$[\Phi]$ = modal matrix
$[\Phi C]$ = modal damping matrix
Ψ = Green's function
ω = frequency of analysis
$[\omega_i^2]$ = diagonal matrix containing the eigenvalues of the structural system

Subscripts

a = point on the BE model
dr = data recovery point

Received March 18, 1997; revision received Nov. 17, 1997; accepted for publication Dec. 23, 1997.

*Assistant Professor, Department of Naval Architecture, 214 NAME Building, 2600 Draper Road.
†Senior Engineering Specialist, P.O. Box 13222.
‡Senior Support Engineer, Software Business Unit, 2805 S. Industrial, Suite 100.

ml = lth integration point of the mth element
r = acoustic pressure due to the rth acoustic wave

Introduction

IN launch vehicle applications it is important to identify the vibration induced on structural components due to the acoustic loads of the launch environment.[1,2] Traditionally, this objective has been achieved by performing testing in a reverberant chamber. The reverberant field is utilized to simulate the launch environment. Acoustic pressure measurements and acceleration measurements are obtained during testing. The acoustic environment in the vicinity of the aft end of a launch vehicle can be extremely high. The overall sound pressure level (OASPL) for Titan IV is predicted to be approximately 166 dB. Typical design margins of 3–6 dB are added to aerospace equipment to reduce the risk of operational failure and to accommodate differences among flight units due to variations in parts, materials, processes, manufacturing, and testing. Within the United States and probably worldwide, capability to meet these test levels does not exist for large parts. Work has been performed in an attempt to achieve these levels.[3] Although high levels were indeed produced (up to 180 dB OASPL), the hardware's response was limited due to high aerodynamic damping imposed by the test fixture.[4] Methods to certify flight hardware[5] that relied on testing at low levels (152–162 dB) and scaling the results to predict responses at the higher levels required for hardware certification were subsequently developed and used successfully. Whereas favorable results have been obtained with the preceding methods, program schedule restraints typically require production hardware to be built in parallel with the qualification hardware. Therefore, it is important for a structural dynamic simulation capability to be available during the initial conceptual design phases of new products. In this manner the hardware performance can be evaluated, and modifications can be implemented before a prototype is built and significant commitments are made in terms of tooling, materials, and manufacturing. Demanding schedule commitments create a need to produce flight capable hardware in as little as one pass. This objective can be accommodated by developing a set of computational tools that can predict the structural capabilities of hardware subjected to high-level acoustic loads. This success-oriented approach has been the prime motivation for developing the formulation presented in this paper. It documents the development of specialized numerical algorithms based on the boundary element (BE) and the finite element (FE) methods for vibroacoustic analyses and their applications in simulating the noise-induced vibration of a component of a launch vehicle.

The BE method has been used in predicting the noise emitted from vibrating structures or the noise generated inside acoustic cavities.[6–15] In such applications the objective is to compute the emitted noise and possibly implement design modifications to reduce it. In this work, however, the effort is concentrated on computing the noise-induced vibration of a structural component due to acoustic loading and on validating the methodology. Two numerical capabilities are important to utilize these numerical tools for industrial launch vehicle applications: 1) accommodating the unequal mesh density between the structural FE model and the acoustic BE model and 2) simulating a reverberant acoustic field as excitation.

The algorithms presented in this work include development work in both areas. They were implemented into software and were utilized to compute the vibration induced on the nozzle of a rocket engine due to reverberant acoustic excitation (Fig. 1). Finally, the numerical results were compared with test data collected in a reverberant chamber test. The indirect BE approach[16,17] is used for the acoustic analysis. It accounts for acoustic medium on both sides of the BE model and allows it to include openings. In this application, air exists on both sides of the cone used in the test (Fig. 1), and one of its sides is open. A coupled structural-acoustic formulation is utilized in the numerical simulation. It allows computation of the acoustic field around the cone and the structural vibration simultaneously. The coupled formulation also handles the acoustic load exerted on the structure and the effect of the structure on the acoustic field.

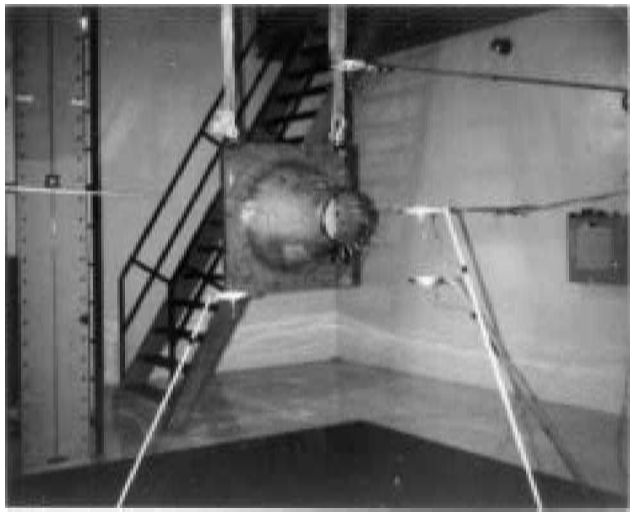

Fig. 1 Testing fixture used in the project.

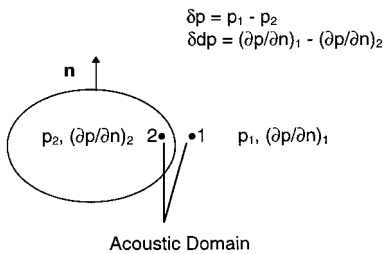

Fig. 2 Definition of primary variables in indirect BE: n = unit normal directed toward domain 1 or 2; δp, δdp = primary variables on the BE model.

Mathematical Background

The BE approach is used to simulate the acoustic medium. The FE method is used to simulate the dynamic behavior of the structure. The main contributions of this work were the development of an algorithm for the coupled structural-acoustic analysis permitting unequal discretization between the BE and FE models and the numerical simulation of the reverberant field as acoustic excitation. A brief introduction to the indirect BE method is presented first. It will identify the important aspects of the BE approach utilized in the development of the coupled algorithms.

Acoustic BE Indirect Method

In the indirect BE method, the difference in the acoustic pressure δp and the difference in the normal gradient of the pressure δdp between the two sides of the model comprise the primary acoustic variables (Fig. 2).[16,17]

By taking into account 1) the Helmholtz integral equation,[10,18,19] containing the acoustic pressure and acoustic velocity for each side of the model, 2) the definition of the unit normal along the two sides of the surface, and 3) the definition of the primary variables on the boundary, the acoustic response at a data recovery point can be expressed as

$$p(\boldsymbol{r}_{\mathrm{dr}}) = \int_S \left[\delta p(\boldsymbol{r}_a) \frac{\partial \Psi(\boldsymbol{r}_{\mathrm{dr}}, \boldsymbol{r}_a)}{\partial n_a} - \Psi(\boldsymbol{r}_{\mathrm{dr}}, \boldsymbol{r}_a) \delta dp(\boldsymbol{r}_a) \right] \mathrm{d}S_a \quad (1)$$

In the indirect method a functional is formed, and the unknown primary variables on the surface of the model are computed such that they extremize the functional, subject to the same boundary conditions as the original differential equation.[20] To assemble the functional, the data recovery point is positioned on the BE model. The value of the velocity is expressed as an integral of the unknown primary variable δp over the surface of the model:

$$-i\rho\omega v(\boldsymbol{r}_b) = \int_{S_a} \delta p(\boldsymbol{r}_a) \frac{\partial^2 G(\boldsymbol{r}_a, \boldsymbol{r}_b)}{\partial n_a \partial n_b} \mathrm{d}S(\boldsymbol{r}_a) \quad (2)$$

A variational principle[20] indicates that the solution to Eq. (3)

$$\Re(\phi) - f = 0 \tag{3}$$

will also minimize the functional presented in Eq. (4),

$$F(\phi) = \int_S \phi \Re(\phi)\, \mathrm{d}S - 2\int_S \phi f\, \mathrm{d}S \tag{4}$$

Applying this variational principle to Eq. (2) results in a symmetric system of equations:

$$[A]\{\delta p\} = \{F_a\} \tag{5}$$

Once the distribution of the primary variables is computed through Eq. (5), the acoustic response at any point within the acoustic space can be computed from Eq. (1).

Coupled Structural-Acoustic Analysis

The coupled analysis combines the structural system of equations with the acoustic system through coupling matrices. In this work a new algorithm has been developed that allows for unequal discretization between the acoustic and the structural model. The coupled matrices are derived from the following physical principles: 1) the acoustic pressure exerts a load on the structure, and 2) the structural velocity defines the acoustic velocity on the boundary (Fig. 3). The matrix equation for the coupled system of equations can be written as

$$\begin{bmatrix} -\omega^2[M] + i\omega[C] + [K] & [C_2] \\ [C_1] & [A] \end{bmatrix} \begin{Bmatrix} \{u_{\mathrm{St}}\} \\ \{\delta p\} \end{Bmatrix} = \begin{Bmatrix} \{F_{\mathrm{St}}\} \\ \{F_a\} \end{Bmatrix} \tag{6}$$

The terms of matrix $[C_1]$ are derived by taking into account the relationship of the structural displacement $\boldsymbol{u}_{\mathrm{ST}}$ of the vibration to the acoustic velocity v_a:

$$i\omega \boldsymbol{u}_{\mathrm{St}} \boldsymbol{n} = v_a \tag{7}$$

When the expression of the acoustic velocity is introduced into the variational functional of Eq. (4) [by taking into account that $f = -i\rho\omega v_a(\boldsymbol{r}_b)$], the corresponding integral associated with the acoustic forcing function represented by the velocity boundary conditions becomes

$$\int_S -i\rho\omega i\omega \boldsymbol{u}_{\mathrm{St}} \boldsymbol{n} \delta p\, \mathrm{d}S = -\rho\omega^2 \int_S \boldsymbol{u}_{\mathrm{St}} \boldsymbol{n} \delta p\, \mathrm{d}S \tag{8}$$

Therefore, the terms of the coupling matrix $[C_1]$ are derived by the integral

$$-\rho\omega^2 \int_S \boldsymbol{u}_{\mathrm{St}} \boldsymbol{n} \delta p\, \mathrm{d}S \rightarrow [C_1] \tag{9}$$

Similarly the terms of the coupling matrix $[C_2]$ are derived by taking into account the force exerted by the acoustic medium on the structure:

$$\mathrm{d}\boldsymbol{F} = (p_2 - p_1)\boldsymbol{n}\, \mathrm{d}S = -(p_1 - p_2)\boldsymbol{n}\, \mathrm{d}S = -\delta p \boldsymbol{n}\, \mathrm{d}S \tag{10}$$

Therefore, by taking into account that the acoustic force exerted on the structure moves to the left-hand side of Eq. (6), it can be concluded that the terms of $[C_2]$ are derived as

$$\int_S \delta p \boldsymbol{n} \boldsymbol{u}_{\mathrm{St}}\, \mathrm{d}S \rightarrow [C_2] \tag{11}$$

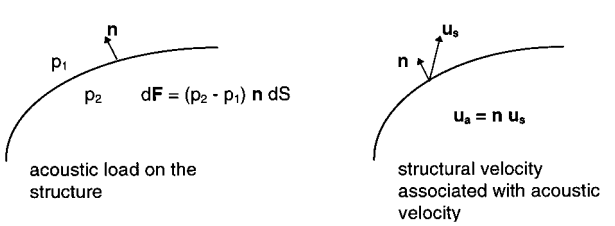

Fig. 3 Structural-acoustic interaction.

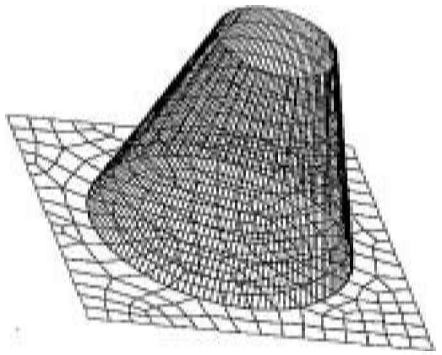

Fig. 4 Structural FE model used in the analysis.

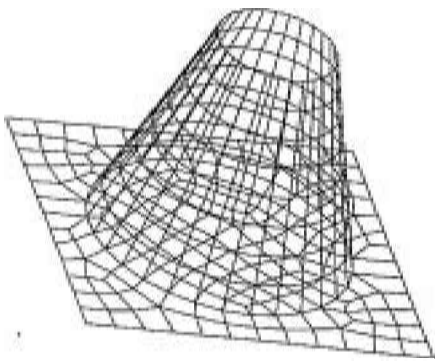

Fig. 5 Acoustic BE model used in the analysis.

In practical applications, the discretizations for the structural and the acoustic model are unequal. Therefore, the number of nodes and elements used to represent the surface S in Eq. (9) is different from the number of nodes and elements used to represent the same surface in Eq. (11). The structural FE model is usually finer than the acoustic BE model. (Figures 4 and 5 present the FE and the BE models, respectively, for the application presented in this work.) To accomplish the derivation of the coupling matrices between the unequal discretization of the structural and the acoustic model, the following procedure is followed. Because the structural FE model is usually the finer one of the two, both integrals from Eqs. (9) and (11) are computed based on the discretization of the structural model. From Eqs. (9) and (11) it can be concluded that

$$[C_1] = -\rho\omega^2 [C_2] \tag{12}$$

The integral that must be computed becomes

$$C = \int_{S_{\mathrm{St}}} \delta p \boldsymbol{n} \boldsymbol{u}_{\mathrm{St}}\, \mathrm{d}S \tag{13}$$

By taking into account that $M =$ number of elements in the FE model and $L =$ number of integration points used within each element, the integral C becomes

$$C = \int_{S_{\mathrm{St}}} \delta p \boldsymbol{n} \boldsymbol{u}_{\mathrm{St}}\, \mathrm{d}S = \sum_{m=1}^{M} \sum_{l=1}^{L} |J_{ml}| w_{ml} \boldsymbol{n}_{ml} \boldsymbol{u}_{\mathrm{St}}(x_{ml}) \delta p(x_{ml}) \tag{14}$$

The structural displacement at point x_{ml} can be represented in terms of the nodal values associated with the K_m nodes of element m:

$$\boldsymbol{u}_{\mathrm{St}}(x_{ml}) = \sum_{k=1}^{K_m} N_k^m(l) \boldsymbol{u}_{\mathrm{St}}(k, m) \tag{15}$$

The quantity $\delta p(x_{ml})$ is computed as

$$\delta p(x_{ml}) = \sum_{i=1}^{K_m} N_i^m(l) \delta p(i, m) \tag{16}$$

Because there is an unequal discretization between the structural and the acoustic model, $\delta p(i, m)$ is expressed in terms of the values of the primary variable δp at the R_i^m closest nodes of the acoustic model to the ith node of structural element m. Therefore,

$$\delta p(i, m) = \frac{\sum_{j=1}^{R_i^m} \delta p(j)/d_j}{\sum_{j=1}^{R_i^m} 1/d_j} \tag{17}$$

By combining Eqs. (14–17), the integral C becomes

$$C = \sum_{m=1}^{M} \sum_{l=1}^{L} |J_{ml}| \boldsymbol{w}_{ml} \boldsymbol{n}_{ml} \sum_{k=1}^{K_m} N_k^m(l) \boldsymbol{u}_{\mathrm{St}}(k, m) \times \sum_{i=1}^{K_m} N_i^k(l) \frac{\sum_{j=1}^{R_i^m} \delta p(j)/d_j}{\sum_{j=1}^{R_i^m} 1/d_j} \tag{18}$$

Therefore, both coupling matrices can be generated between the unequal discretizations of the FE and BE models. In addition, the coupling algorithm is general enough to allow, if necessary, for only a certain portion of the acoustic model to interface with the structural model. On the remaining, acoustic boundary conditions can be assigned as part of the acoustic excitation.

In the numerical approach used to solve Eq. (6), the structural degrees of freedom are expressed as a linear superposition of the normal modes. Through partitioning and condensation techniques, Eq. (6) is reduced to a system equal to the acoustic system of equations. This includes the effect from the structural-acoustic interaction and the mechanical load, which might be applied on the structure:

$$\left[[A] - [C_1][\Phi]\left[-\omega^2[I] + i\omega[\Phi C] + \left[\omega_i^2\right]\right]^{-1}[C_2]\right]\{\delta p\} = \{F_a\} - [C_1][\Phi]\left[-\omega^2[I] + i\omega[\Phi C] + \left[\omega_i^2\right]\right]^{-1}[\Phi]^T\{F_{\mathrm{St}}\} \tag{19}$$

The solution to Eq. (19) results in computation of the primary acoustics variables on the surface of the model. It includes the effect from the acoustic loading (acoustic sources and/or acoustic velocity or pressure boundary conditions), the structural vibration, and the structural mechanical load. Once the primary variables are computed, the modal degrees of freedom can be evaluated, and sequentially the structural vibration can be computed.

Numerical Modeling of the Reverberant Acoustic Field

One of the main challenges of utilizing a BE/FE approach in simulating the vibration induced from a launch environment has been the numerical representation of the reverberant field that comprises the excitation in the current testing procedures. The reverberant field can be considered to be generated by a large number of waves traveling in all directions with a random phase. Therefore, the magnitude of the acoustic pressure at any point of such a field and the energy are constant. In this work, the approach employed to generate the reverberant field is to utilize multiple-plane acoustic wave sources acting as independent excitations and adding their effects on energy basis. The origins of the plane waves are defined on the surface of an imaginary sphere surrounding the structure. The radius of it is equal to 20 times the main dimension of the structure. The direction of all of the waves is toward the center, and the origins are equally spaced over the imaginary surface. In this manner there are several plane waves acting at each point of the acoustic field, and acoustic excitation is applied on the structure from every possible direction. Because in a reverberant field the mean square pressure is proportional to the power of the field,[21] results obtained by the individual plane wave excitations are summed up on energy basis. Therefore, at a particular point within the acoustic field the acoustic response is

$$p_{\mathrm{tot}}^2 = \sum_{r=1}^{RV} p_r^2 \tag{20}$$

Similarly, the vibration induced on the structure from the acoustic field is computed as

$$u_{\mathrm{Stot}}^2 = \sum_{r=1}^{RV} u_{\mathrm{Sr}}^2 \tag{21}$$

Because the number of individual analyses is equal to the number of plane waves required to simulate the reverberant excitation, special attention is necessary to minimize the number of computations performed. Specifically, during solution of Eq. (19), only the right-hand side of the equation changes due to multiple forcing excitations originating from each one of the plane waves. That is taken into account during the solution, and only backsubstitution is performed multiple times for each one of the forcing functions.

Application

The coupled structural-acoustic formulation presented in the preceding section was utilized in computing the noise-induced vibration on an expansion nozzle of a rocket engine. Aerojet is a supplier of chemical rocket propulsion systems. These systems use expanding nozzles to direct the combustion products and to increase engine thrust. It was decided to manufacture a test specimen similar in size, material, and configuration to an actual production nozzle. Although the entire validation process, including analytical and manufacturing considerations, would have been simpler with a flat panel, the more complex nature of flight-like structure lends more confidence to the technique upon a good match.

The validation hardware is similar in size, shape, material, and manufacture to a nozzle Aerojet currently provides on its Titan IV stage I liquid rocket engine as a thrust enhancer. It is attached via butt welds to a fluid heater assembly, which is utilized to produce oxidizer tank pressurant gases. It further expands the hot gases that are used as prime movers of the high-speed turbopumps. It differs in the end configurations from the actual production hardware. Although the forward end (smallest diameter of the truncated cone) is welded to the other structure, the validation hardware is free. The large-diameter end of the production unit is attached via butt welds to a relatively thick aft flange that has a complex joint to an exit closure used as a radiation barrier for sensitive heating coils during the portions of flight before engine operation. The exit closure is essentially a flat plate. The validation hardware incorporates a very thick plate at its aft end to attain a nearly infinite stiffness boundary.

Methodology

The following primary steps are needed in calculating the structural response to an acoustic excitation using the developed methodology: 1) construction of an FE model and completion of structural analysis for eigenvalues and eigenvectors, 2) identification of the frequencies for harmonic coupled structural-acoustic analyses, 3) construction of a BE model and completion of an indirect coupled harmonic analysis, and 4) postprocessing of the structural vibration in square acceleration of gravity per hertz. The results can potentially be used in computing the stress and strain for the structure.

During this process the coupling between the acoustic inputs and the structure are handled rigorously. No assumptions about which modes are excited need to be made. Experience shows that structural modes for which geometry and acoustic wavelength do not match have very low participation. Also, modes with small generalized forces such as torsion have low participation. Many structural modes can be included, and the number is practically limited only by workstation capability. There is no trouble handling modes in frequency ranges with low modal density, as is often the case with statistical energy methods.[2] The acoustic BE model can be coarser than the corresponding structural FE model.

The FE model of the validation hardware consists entirely of four-node quadrilateral elements (Fig. 4). Analytical eigenvalues have been verified by tap testing, and response autospectrums obtained during reverberant acoustic testing show excellent correlation to the low-level tap tests. The model was tuned to the extent that all analytical natural frequencies were comparable to measured values up to 1000 Hz. This encompassed 29 analytical flexible body modes including repeated roots. Because the geometry is quite simple and

the materials and thicknesses were well known, model tuning was accomplished by adjusting the number of elements between spot welds. Spot welds between the cone and plate are modeled with an equivalenced single node. More elements produced better results. Four elements per weld yielded eigenvalues to within, at most, 4% of measurement, and no further tuning was performed.

The frequency range of primary interest was between 250 and 500 Hz. Thus, the modal basis includes modes up to 1000 Hz. This specific frequency range was chosen based on past experience in vibroacoustics of nozzles. Overall structural strain for this type of structure will be dominated by the several lowest excitable natural frequencies. These lowest frequencies tend to produce the largest displacements. The BE model was created with fidelity to yield approximately eight nodes for the highest acoustic wavelength of the analysis, 1000 Hz (Fig. 5). Both the cone and plate receive acoustic energy necessitating that both be modeled. The BE model was easily generated with the geometry database created for the FE model. The two models had different meshes, and this was handled by the algorithm described previously.

Testing and Validation

The main dimensions of the nozzle used in the test were diameters of 2 ft at the large end and 10 in. at the small end and a height of 2 ft. The material was stainless steel. Two different tests and simulations were performed for the manufactured hardware. First the fixture was placed in a free field, and a noise source was positioned 14 in. away from the upper edge of the structure. The noise was generated from high-pressure nitrogen coming out from a noise-producing nozzle. Four microphones were positioned around the fixture. They were utilized in characterizing the acoustic excitation. Six accelerometers were mounted at an equal-spaced arrangement along one-quarter of the circumference of the cone and 2 in. away from the upper edge (Fig. 6). In the numerical analysis the noise source was approximated by a quadropole. Its magnitude was calibrated to simulate the measured acoustic pressure. Thus, an equivalent loading on the structure was accomplished between the testing and the simulation. From the coupled structural-acoustic analysis, the vibration induced on the fixture was computed. Results for the measured acceleration and the computed maximum acceleration (square acceleration of gravity per hertz) are presented in Fig. 7. The comparison between the two sets of data was very satisfactory.

1) The same number of peaks was observed at similar frequencies. Each peak corresponded to the first five structural normal modes of the fixture.

2) The maximum values of the peaks were comparable.

3) The values for the highest response (which will result in the highest stress) were within 1 dB.

4) The peak-to-valley ratios were comparable.

Once the initial free field testing and validation were completed, a second test at a reverberant chamber was justified. The dimensions of the chamber were 20 × 20 ft square and 80 ft high. The fixture was positioned in the center of the room, 6 ft from the floor. In this case the acoustic field to which the hardware was subjected is specified as reverberant. Therefore, the sound field is nondirectional, having, theoretically, zero intensity in any direction. It is also diffused, which implies that the sound pressure is the same

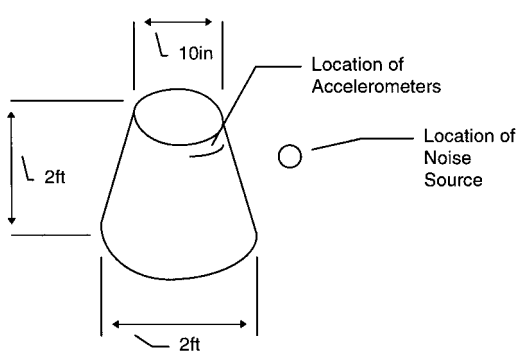

Fig. 6 Test fixture, location of accelerometers, and noise source for free field testing.

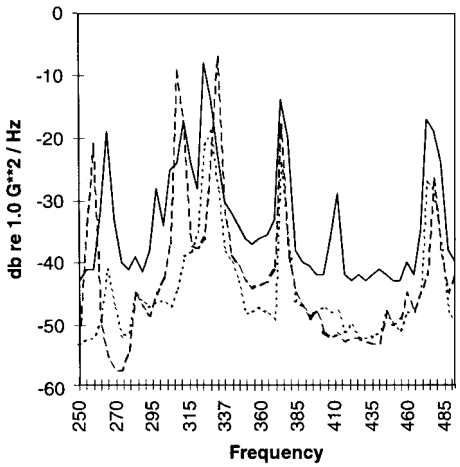

Fig. 7 Correlation between test data and numerical results for free field testing: ——, max test; - - - -, min test; and – – –, max analysis.

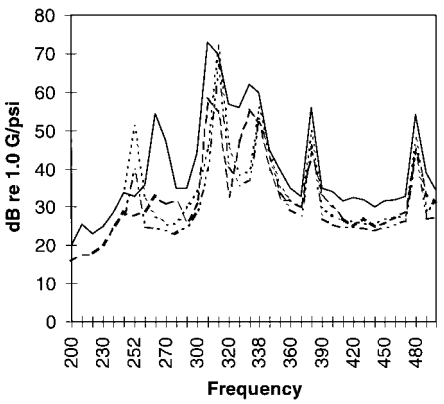

Fig. 8 Correlation between test and analysis: – – –, test min; ——, test max; – – –, analysis min; - - - -, analysis max.

everywhere within the field. The mathematical approach presented earlier was utilized in numerically generating the reverberant field. The acoustic source strengths for each frequency of the analysis can be set to provide the analysis's specification strength. The system being analyzed is classified as open. Therefore, the fluid medium is present on both sides of the BE model and requires an indirect BE formulation. Results (Fig. 8) show verification of the coupled structural-acoustic algorithm and the reverberant field simulation developed in this work. Analytical predictions for the acceleration are obtained by twice differentiating the displacement results normal to the surface and normalizing by the average pressure. Test data were obtained directly with accelerometers and microphones. This presentation permits direct comparison of analytic and test data. Maximum and minimum envelopes, for nodes or measurements, are shown for responses at approximately 1.6 in. from the small-diameter end of the test hardware. This region was chosen for the comparison because it experienced large accelerations in test. The following observations were made.

1) There was good correlation in terms of the number and the frequencies of peak response.

2) The highest peak in the analysis data was within 1 dB of test.

3) All of the computed values of the peaks are within 6 dB from measured data.

4) There was good agreement of peak-to-valley differences, which indicates good matching with respect to damping.

In addition, the acoustic pressures (noise levels) computed around the structure were practically constant, which indicates that a good numerical representation of the reverberant field was achieved.

Conclusions

A capability to simulate the noise-induced vibration on components of a launch vehicle due to acoustic loads is important in

reducing the development time. It allows the analysis of different configurations efficiently through the utilization of computational models. The BE method is a suitable approach for numerical acoustics, and in the application of interest it is utilized in simulating the acoustic field of the launch environment. The FE method can be used to determine numerically the dynamic characteristics of a structure. In this work, a new methodology was developed for the coupling of the structural FE and the acoustic BE methods in solving noise-induced vibration problems associated with launch vehicle applications. The new developments presented here are the unequal mesh density capability between the structural and the acoustic model and the simulation of a reverberant acoustic field as excitation. Both capabilities are important in utilizing the new methodology in launch vehicle applications. An expanding nozzle of a rocket engine was used in the validation of the development. Two tests were performed, and the results were successfully compared with the corresponding numerical simulations. The vibration was measured during an acoustic free field test and also in a reverberant environment. There was good correlation between the maximum measured and computed accelerations, the number and frequencies of peak responses, and the peak-to-valley ratios.

References

[1]Bergen, T. F., Himelblau, H., and Kern, D. L., "CASSINI Spacecraft Acoustic Flight and Test Criteria," *Proceedings of Noise-Con 96*, Noise Control Foundation, New York, 1996, pp. 693–698.

[2]Bradford, L., and Manning, J. E., "Attenuation of the Cassini Spacecraft Acoustic Environment," *Sound and Vibration*, Vol. 10, Oct. 1996, pp. 30–37.

[3]Lieberman, P., Bocksrucker, R., Pilgram, G., and Vallance, C., "Progressive Wave Tube Facility with Additional Capabilities," AIAA Paper 93-0288, Jan. 1993.

[4]Vallance, C. S., and Foss, R. L., "High Intensity Acoustic Testing of a Rocket Engine Ablative Nozzle Extension," *42nd Annual Technical Meeting of the Institute of Environmental Sciences, Design, Test, and Evaluation Proceedings*, AIAA, Reston, VA, 1996, pp. 286–293.

[5]Himelblau, H., Kern, D. L., and Davis, G. L., "Development of Cassini Acoustic Criteria Using Titan IV Flight Data," *Proceedings of the 38th ATM*, Vol. 2, Inst. of Environmental Sciences, 1992, pp. 307–331.

[6]Burton, A. J., and Miller, G. F., "The Application of Integral Equation Methods to the Numerical Solutions of Some Exterior Boundary Value Problems," *Proceedings of the Royal Society of London*, Vol. 323, April 1971, pp. 201–210.

[7]Imai, M., Suzuki, S., Sugiura, N., and Sato, H., "Radiation Efficiency of Engine Structures, Analyzed by Holographic Interferometry and Boundary Element Calculation," Society of Automotive Engineers, SAE Paper 861411, May 1986.

[8]Kirpur, S. M., and Tyrrell, R. J., "Computer-Aided Analysis of Engine Noise," *International Journal of Vehicle Design*, Vol. 13, No. 4, 1992, pp. 388–402.

[9]Koopman, G. H., and Benner, H., "Method for Computing the Sound Power of Machines Based on the Helmholtz Integral," *Journal of the Acoustical Society of America*, Vol. 71, No. 1, 1982, pp. 77–89.

[10]Seybert, A. F., Soenarko, B., Rizzo, F. J., and Shippy, D. J., "Application of the BIE Method to Sound Radiation Problems Using an Isoparametric Element," *Journal of Vibration, Acoustics, Stress, and Reliability in Design*, Vol. 106, Oct. 1984, pp. 414–420.

[11]Smith, D. C., "Noise Control Design of Vibrating Structures Using the Boundary Element Method," M.S. Thesis, Mechanical Engineering Dept., Purdue Univ., West Lafayette, IN, 1988.

[12]Smith, D. C., and Bernhard, R. J., "An Experimental Verification of Numerical Techniques Based on the Helmholtz and Rayleigh Integral Equations," *Proceedings Noise-Con 88*, Noise Control Foundation, New York, 1988, pp. 615–620.

[13]Suzuki, S., Maruyama, S., and Ido, H., "Boundary Element Analysis of Cavity Noise Problems with Complicated Boundary Conditions," *Journal of Sound and Vibration*, Vol. 130, Jan. 1989, pp. 79–91.

[14]Utsumo, H., Tanaka, T., Inoue, K., and Nishibe, M., "Analysis of the Sound Field in an Automotive Cabin by Using Boundary Element Method," Society of Automotive Engineers, SAE Paper 891153, May 1989.

[15]Vlahopoulos, N., Shalis, E. V., and Latcha, M. A., "A Numerical Approach for the Prediction and Reduction of Structure-Borne Noise During the Design Stage of Ground Vehicles," *Proceedings of 14th ASME Biennial Conference on Mechanical Vibration and Noise*, American Society of Mechanical Engineers, New York, 1993, pp. 73–80.

[16]Brebbia, C. A., Telles, J. C. F., and Wrobel, L. C., *Boundary Element Techniques, Theory and Applications in Engineering*, 1st ed., Springer–Verlag, New York, 1984, pp. 58–60.

[17]Lamb, H., *Hydrodynamics*, 6th ed., Dover, New York, 1932, pp. 113–115.

[18]Chertock, G., "Sound Radiation from Vibrating Surfaces," *Journal of the Acoustical Society of America*, Vol. 36, No. 7, 1964, pp. 1305–1313.

[19]Cickowski, R. D., and Brebbia, C. A. (eds.), *Boundary Element Methods in Acoustics*, Computational Mechanics Publications, Southampton, England, UK, and 1st ed., Elsevier Applied Science, London, 1991, pp. 61–74.

[20]Mikhin, S. G., *Variational Methods in Mathematical Physics*, Macmillan, New York, 1964, pp. 72–75.

[21]Cremer, L., Heckl, M., and Ungar, E. E., *Structure-Borne Sound, Structural Vibrations and Sound Radiation at Audio Frequencies*, 1st ed., Springer–Verlag, New York, 1973, pp. 506–520.

H. L. McManus
Associate Editor